Multimodality localization of epileptic foci

M Desco[a], J Pascau[a], MA Pozo[c], A Santos[b], S Reig[a], J Gispert[a], P García-Barreno[a]

[a] Hospital General Universitario 'Gregorio Marañón', E-28007 Madrid (Spain)
[b] Universidad Politécnica de Madrid, E-28040 Madrid (Spain)
[c] Instituto Pluridisciplinar. Universidad Complutense de Madrid, E-28040 Madrid (Spain)

ABSTRACT

This paper presents a multimodality approach for the localization of epileptic foci using PET, MRI and EEG combined without the need of external markers.

Mutual Information algorithm is used for MRI-PET registration. Dipole coordinates (provided by BESA software) are projected onto the MRI using a specifically developed algorithm. The four anatomical references used for electrode positioning (nasion, inion and two preauricular points) are located on the MRI using a triplanar viewer combined with a surface-rendering tool. Geometric transformation using deformation of the ideal sphere used for dipole calculations is then applied to match the patient's brain size and shape.

Eight treatment-refractory epileptic patients have been studied. The combination of the anatomical information from the MRI, hipoperfusion areas in PET and dipole position and orientation helped the physician in the diagnosis of epileptic focus location. Neurosurgery was not indicated for patients where PET and dipole results were inconsistent; in two cases it was clinically indicated despite the mismatch, showing a negative follow up.

The multimodality approach presented does not require external markers for dipole projection onto the MRI, this being the main difference with previous methods. The proposed method may play an important role in the indication of surgery for treatment-refractory epileptic patients.

Keywords: multimodality, registration, fusion, epilepsy, EEG, positron emission tomography, PET, magnetic resonance imaging, MRI, neurosurgery

1. INTRODUCTION

The accurate location of epileptic foci in treatment-refractory epileptic patients is an important issue as it determines the diagnosis and influences the decision of applying surgical treatment. Epileptic foci are identified with a good temporal resolution using non-invasive scalp recorded EEG signals, but these recordings have very poor spatial resolution and their relation to the underlying brain anatomy is not obvious. The analysis of EEG data is performed calculating magnetic dipoles on spherical or elliptical models of the patient's head [1-3]. With them a rough idea of the position of the dipoles on the brain of the patient can be obtained.

However, in order to obtain a more accurate localization of the dipoles, their position must be identified on 3D Magnetic Resonance Images (MRI) [4-9] where anatomical information has much higher resolution. Complementary information about activity or metabolism, such as that provided by Positron Emission Tomography (PET) is also important to validate the location of abnormal electrical activity provided by the dipole and head models. In this way, focal epileptogenic activity may be related to brain lesions observed in MRI and brain hipometabolism visualized with PET.

Correspondence: Dr. M. Desco. Hospital General Universitario "Gregorio Marañón". c/ Dr. Esquerdo, 46. E-28007. Madrid. SPAIN. e-mail: desco@mce.hggm.es http://www.hggm.es/image.

Medical Imaging 2001: Physiology and Function from Multidimensional Images, Chin-Tu Chen, Anne V. Clough, Editors, Proceedings of SPIE Vol. 4321 (2001) © 2001 SPIE · 1605-7422/01/$15.00

Registration of dipole locations with MRI and/or PET volumes has been achieved using external skin markers visible in MRI (and possibly PET) images, placed on the locations that correspond to the EEG electrodes [4, 6, 9, 10], or on some of the anatomical landmarks that define the 10-20 reference system [11-13]. These points are easily identified on MRI volumes and allow for the dipole projection on these images.

However, the use of external markers has several drawbacks. Sometimes, previously acquired MRI are available but cannot be used if they do not include the markers. In other cases, the PET, MRI or EEG acquisitions are performed at different facilities and/or dates, making difficult or even impossible the use of the same external markers. For these cases and also for reasons of patient comfort and simplicity of the acquisition protocols, the registration of MRI, PET and EEG data for the dipole localization without marker facilities seems very convenient.

The method presented here employs the maximization of Mutual Information algorithm [14, 15] for the registration of PET and MR images without markers. The coordinates of the dipoles that model the EEG recording are then projected onto the MR image without the need of external markers. Our approach is based on the identification of the anatomical landmarks that define the 10-20 reference system using 3D tri-planar views and surface rendering of the MR. This method has been tested on several patients and provides a way to link the EEG dipole locations to their underlying anatomy. As these patients are candidates to surgical treatment, the contribution of this process may be a significant support to other imaging techniques that do not always provide definitive results.

2. MATERIALS AND METHODS

The study group includes eight treatment refractory epileptic patients. In this work we have studied their MRI (T1 or T2 weighted sequences), PET scan and EEG dipole localization.

2.1. EEG acquisition and source localization

EEG electrode positioning followed the 10-20 International System of Electrode Placement. EEG activity was recorded with a 62-channel Neuroscan equipment (Neuroscan Labs, Sterling, USA), using a common average reference. EEG activity was recorded for 15 to 20 min in resting conditions with the eyes closed, and digitally filtered below 2Hz and above 20 Hz.

The recorded epileptiform discharges were identified by visual inspection of EEG in search of interictal spikes or sharp waves. EEG epochs of 1024 ms centered on the negative peak of the discharge were collected and averaged (range 36 to 180 epochs).

Brain Electric Source Analysis software (BESA v.2.2 from MEGIS Software GmbH, Munich, Germany) was used for dipole source modeling. This program uses a simple four-shell spherical head model, with the shells representing the brain, cerebrospinal fluid (CSF), skull and scalp [3, 16]. The thickness and conductivities of the layers required by the model were: 70 mm for the cortical surface radius, 72 mm for CSF, 7 mm for skull thickness and 6 mm for scalp, being 85 mm the outer layer sphere radius. Conductivities were 0.33, 1.0, 0.0042 and 0.33 mhos/m for brain, CSF, skull and scalp respectively.

Spatio-temporal fixed dipole modeling was performed according to following strategy:
A. A first dipole fitting was performed for the whole epochs of 1024 ms.
B. A second fitting was constrained to the epoch of the spike itself (51-108 ms) at the same location.
A residual variance smaller than 10% was considered an appropriate fit.

With these model parameters, BESA software calculates an equivalent dipole at the appropriate location within the electrical head model described above. This process is guided by the operator, who formulates hypothesis about the number of sources and their location. The solution found by the program consists of one or several dipoles with their origin, orientation and moment expressed in the 10-20 coordinate system. These sources are drawn on the spherical head model, giving a rough estimation of their anatomical position (**Figure 1**).

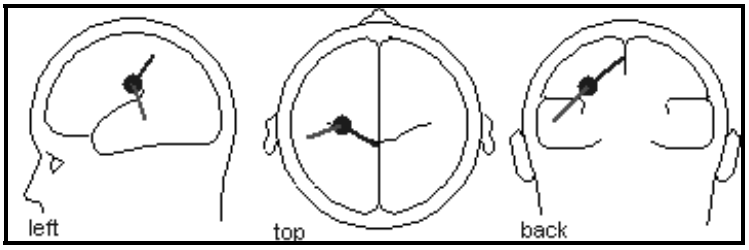

Figure 1. Standard graphical output of BESA software for source location (four-shell head model)

2.2. MR-PET registration

The algorithm used in this step is based on the maximization of Mutual Information (MI) initially proposed by [14] and [15]. Mutual Information is a concept taken from information theory that represents the degree of dependence of two random variables *A* and *B* by measuring the distance between the joint distribution $p_{AB}(a,b)$ and the distribution associated with the case of complete independence $p_A(a) \cdot p_B(b)$ [14]. This concept is related to the entropy of the random variables by the equation:

$$I(A,B) = H(A) + H(B) - H(A,B) = H(A) - H(A \mid B) = H(B) - H(B \mid A) \quad (1)$$

where $I(A,B)$ represents the mutual information between *A* and *B*. $H(A)$ and $H(B)$ are the entropies of these random variables, $H(A,B)$ their joint entropy, and $H(A|B)$ and $H(B|A)$ the conditional entropies. The entropy provides information on the amount of uncertainty about a random variable; $I(A,B)$ is the reduction of uncertainty of a random variable *A* by the knowledge of another variable *B*. The entropies are calculated as:

$$H(A) = -\sum_a p_A(a) \cdot \log_2 p_A(a) \qquad H(A,B) = -\sum_{a,b} p_{AB}(a,b) \cdot \log_2 p_{AB}(a,b) \quad (2)\ (3)$$

Working with images, the probability density function can be estimated by the histogram, usually very easy to obtain. The optimum geometrical transformation *T* that registers two images will maximize the information of one image that is explained by the other. If *B* is the image to be transformed and *A* is the reference, the aim of the algorithm is to find *T* that maximizes $I(A,T(B))$. Then the calculation of the registration corresponds to the maximization of MI depending on the parameters that describe the transformation. As in our study both images come from the same patient, the registration consists of a rigid body transformation (6 parameters: rotations around the three axis and three translations). For the calculation of the joint histogram we have followed [14], that estimates the joint histogram $H(A,T(B))$ using partial volume interpolation. This interpolation scheme does not create new intensity values in every iteration of the optimization, improving the accuracy of the results as compared to nearest neighbor or trilinear interpolation.

A multiresolution approach has been used to maximize $I(A,T(B))$. This method improves the speed of the search and the stability of the resulting transformation. The six parameters (three translations and three rotations) are calculated with progressive user selectable subsampling steps in the range 884, 442, 221, 111 (X, Y and Z subsampling). 442 and 221 steps were used in all the cases providing accurate results. The optimization strategy chosen was Simplex algorithm [17] that, according to [18], is a good compromise between speed and simplicity of implementation since it does not require evaluation of the MI gradient. The solution was found in 4 minutes on average on a standard PC workstation (Intel PIII 800 MHz., 256 Mb RAM). MR was the reference volume in all the cases, and PET scan was transformed to fit MR dimensions.

2.3. Dipole projection onto MRI coordinate system

Once MR image and PET scan are registered, same coordinates in both images represent same geometrical location on the patient's head. Transferring the dipole onto the MR image implies that the three modalities will be co-registered.

The coordinate axis were calculated in the MRI using the four anatomical landmarks that define the 10-20 International System: nasion (N), inion (I) and both pre-auricular points (PreL and PreR). A specific application was developed to find the positions of these points in the MRI. A skin surface rendering combined with a triplanar 3D viewer allowed the user to manually identify these references (**Figure 2**).

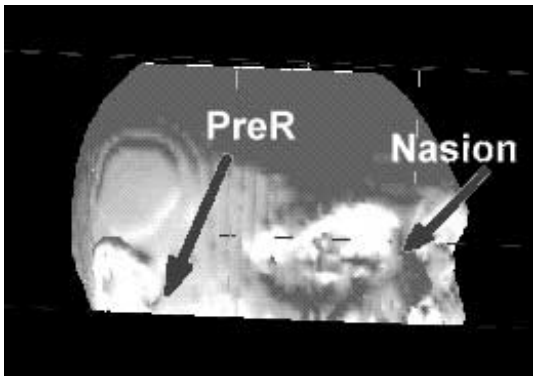

Figure 2. Two landmarks identified on the MRI surface rendering.

Once the four landmarks are set, the dipole coordinate system can be determined. First, the three unitary vectors are calculated: v^{NI} from inion to nasion, v^{LR} from the right pre-auricular point to the left one, and v^{CZ} from the middle point of the segment nasion-inion being perpendicular to the other two. During EEG acquisition, and according to the 10-20 coordinate system, the electrodes were positioned dividing both N-I and PreL-PreR half circumferences in 10 parts. For that reason, at 18 degrees (180/10) steps starting from N, I, PreL and PreR we locate the electrodes Frontal Pole (FP), Occipital Pole (OP), T7 and T8. Theoretically, the center of the electrodes sphere should be the crossing point of the lines PF-OP and T7-T8. If these lines do not intersect, the sphere center is set at the point with minimum distance to both lines (**Figure 3**). The sphere center should be near the bottom of the third ventricle, and about 5 mm. anterior to the posterior commissure [10]. In all the cases, this issue helped the operator in the decision about the accuracy in the selection of the four 10-20 system references. If the sphere center was not centered in the image and far away from the described location, the reference selection was repeated before proceeding.

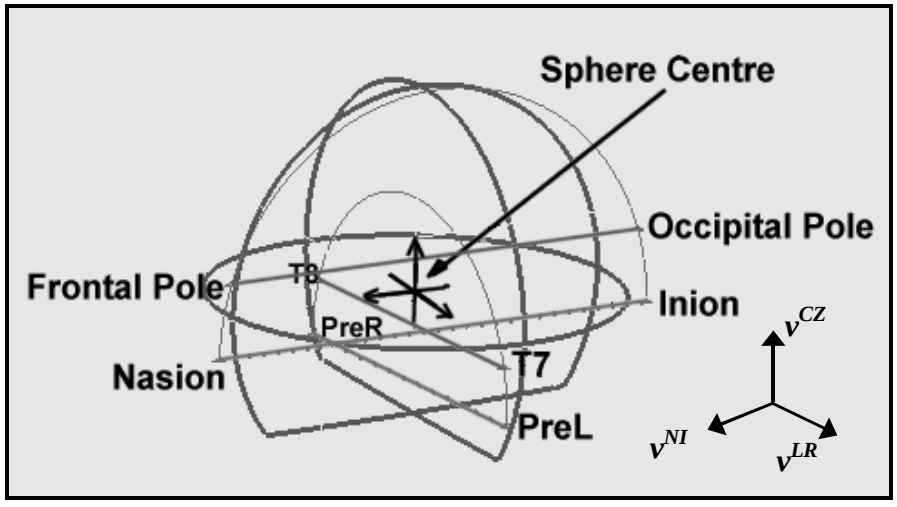

Figure 3. The dipole coordinate system calculated from the four 10-20 anatomical references, (nasion, inion and pre-auricular points), showing the unit vectors and the sphere centre.

The dipole data provided by BESA (Cartesian coordinates *x*, *y* and *z*) are transferred onto the MRI using the coordinate system defined by the unitary vectors and the sphere center. The outer sphere has a radius of 85 mm in the BESA four-shell head model. This simple model is then adjusted to the patient's actual head dimensions. Dipole coordinates are scaled to the *x*, *y* and *z* radius measured from the center of the sphere in the MRI. The method is summarized in equation 4, and figure 4 shows an example of the result.

$$\begin{bmatrix} D'_x \\ D'_y \\ D'_z \\ 1 \end{bmatrix} = \begin{bmatrix} v_x^{NI} & v_y^{NI} & v_z^{NI} & C_x \\ v_x^{LR} & v_y^{LR} & v_z^{LR} & C_y \\ v_x^{CZ} & v_y^{CZ} & v_z^{CZ} & C_z \\ 0 & 0 & 0 & 1 \end{bmatrix} \cdot \begin{bmatrix} s_x & 0 & 0 & 0 \\ 0 & s_y & 0 & 0 \\ 0 & 0 & s_z & 0 \\ 0 & 0 & 0 & 1 \end{bmatrix} \cdot \begin{bmatrix} D_x \\ D_y \\ D_z \\ 1 \end{bmatrix}$$

$$D \equiv Dipole\ coordinates\ in\ 10\text{-}20\ system$$

$$D' \equiv Dipole\ coordinates\ in\ MRI\ system \qquad (4)$$

$$v^{NI}, v^{LR}, v^{CZ} \equiv Unitary\ vectors\ from\ 10\text{-}20\ system$$

$$C \equiv Sphere\ centre\ (10\text{-}20\ system\ origin)$$

$$s_x = \frac{r_x}{85}, s_y = \frac{r_y}{85}, s_z = \frac{r_z}{85} \quad Scale\ factors$$

$$r_x, r_y, r_z \equiv Head\ radii\ measured\ from\ C$$

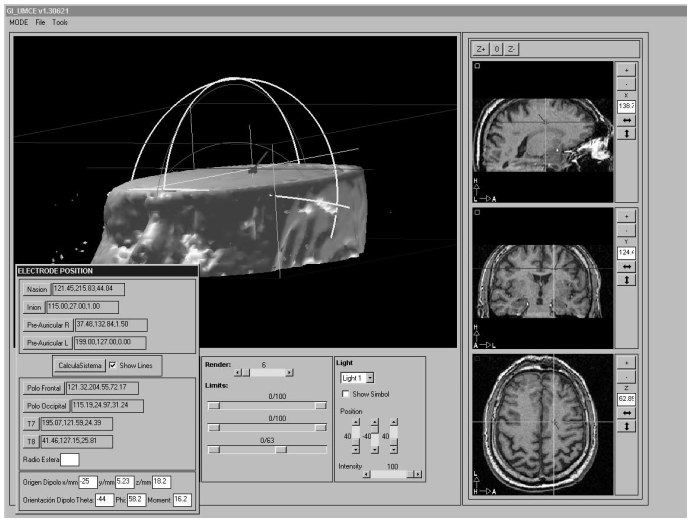

Figure 4. Dipole projection onto the patient's MRI and the sphere used in the electrical head model.

2.4. Image fusion

When PET and EEG are registered to the MRI, the three modalities can be displayed together to help the physician in the decision about the appropriate surgical indication for the patient. Several image fusion tools are available for this step: curtain mode is very useful to check image registration accuracy, while color fusion is able to show the combined information of the three modalities together in one image (**Figure 5**).

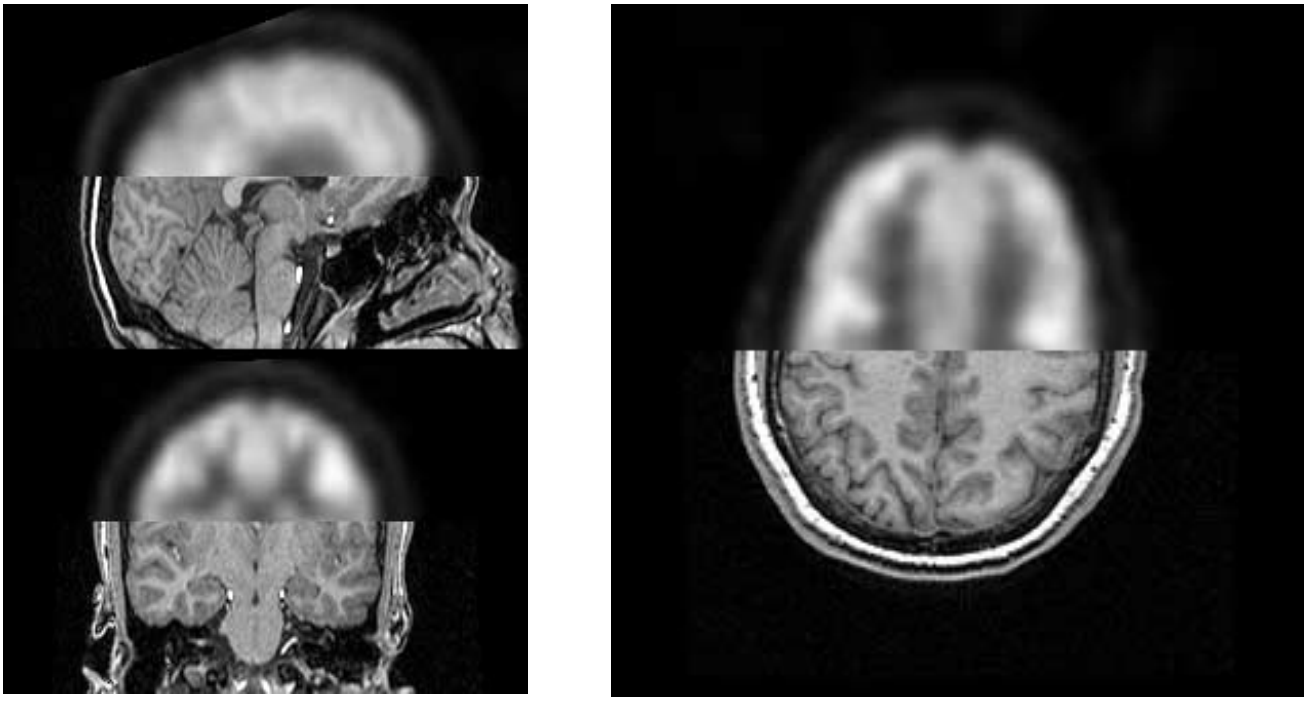

Figure 5. *Curtain mode* visualization tool is used to check the quality of the registration process.

3. RESULTS AND DISCUSSION

The dipole location in relation with the underlying anatomy was studied in eight patients. For all the patients, the dipole was projected onto the MRI and PET scan was registered to the MRI according to the described methods. The physician compared the location of dipoles and hipoperfusion areas obtained from the PET. MRI provided the anatomical structure underlying these areas, and in some patients showed pathological abnormalities (**Figure 6** and **Figure 7**). In six patients, the combined information was consistent and surgery was indicated. The postoperative follow-up showed a decrease in the epileptic attacks, evaluating the outcome of the intervention as positive for those patients. The combined techniques didn't match in two cases, and the decision was made on the basis of the PET results, despite the different dipole location. These patients were also operated but the follow-up did not show significant improvement.

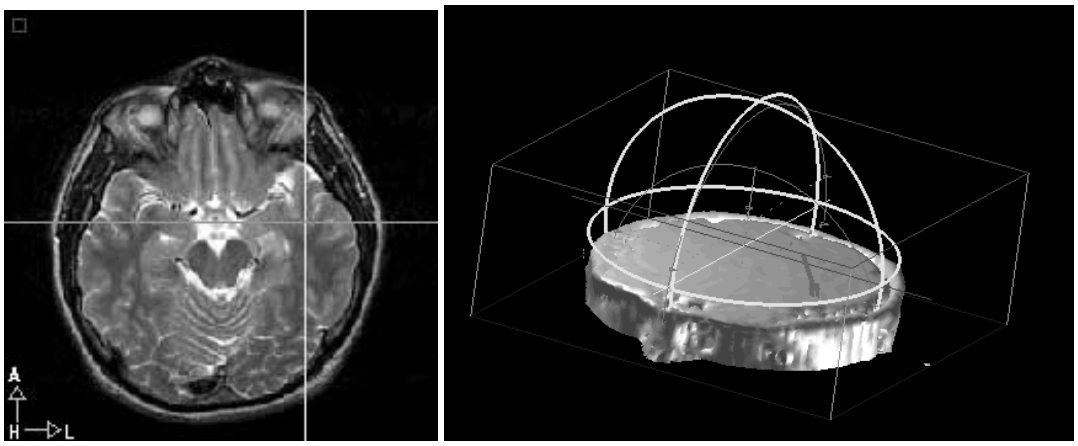

Figure 6. Dipole location results on a patient's MRI. The dipole appears in a Left Temporal area.

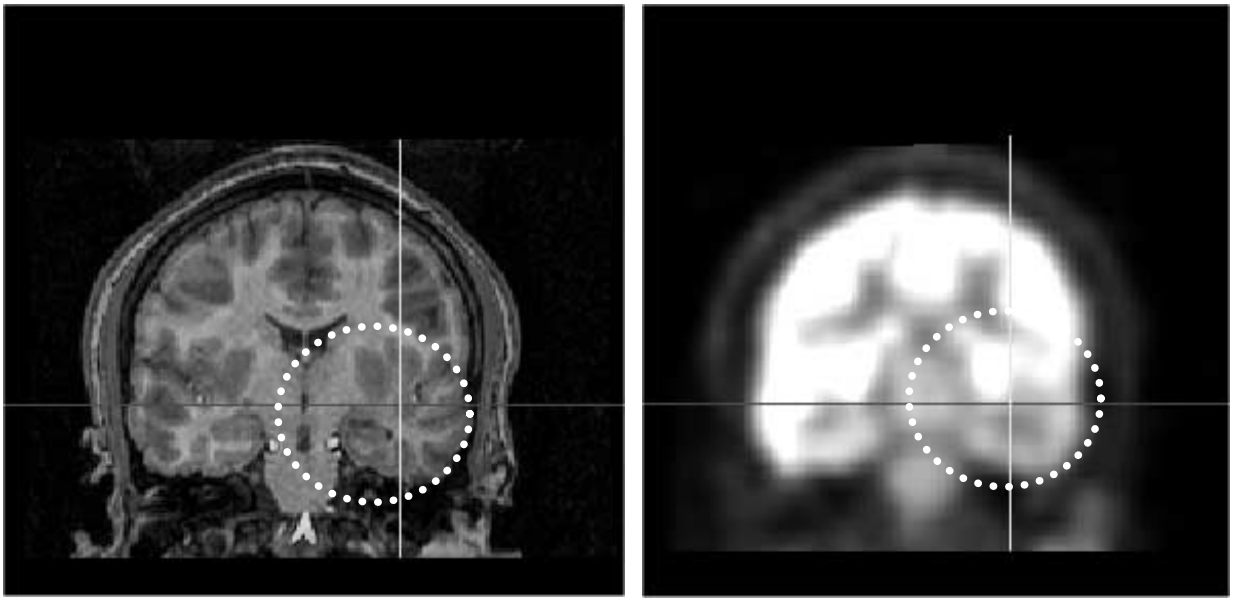

Figure 7. Axes cross on the dipole position provided by BESA and transferred to the MRI and PET. Mesial sclerosis is visible on the MR image (*left*) in the area where the dipole is located. PET asymmetry in that area is also clearly visible (*right*).

The results show that this technique may be useful for checking the anatomical origin of the EEG source location, improving the rough dipole positioning provided by BESA. The manual identification of the four 10-20 system anatomical references seems to be accurate enough to locate the dipole on the MRI, according to clinical criteria. The MRI-PET registration provides also complementary information to the physician.

A limitation of our work is that no objective assessment of the method accuracy can be obtained, since there is no 'gold standard technique' to compare with. On the other hand, the BESA approximations are reported to yield errors in the range of 1-2 cm due to the approximations that support the four sphere model[1, 2, 19]. For this reason, only clinical evaluation of the results can be provided.

The goal of depicting the dipole position together with the MRI anatomical data and PET functional information is clinically very interesting. As an alternative to the described method, several authors propose the use of patient's MRI to improve the calculation of dipole position [7]. There is also a commercial package – CURRY® from Neuro Scan Labs –, that using the electrode position information obtained from external markers, solves the EEG inverse problem in a realistic head model[20]. These methods do not avoid however the registration of the electrodes location to the MRI, although they seem to be the best technical solution for EEG source localization.

As a difference with other approaches based on external markers, our procedure can be used either in prospective or retrospective way. This overcomes the problem of obtaining the MRI image with the external markers, and allows for the use of almost any MRI diagnostic study of the patient, acquired before or after the EEG.

As a conclusion, the results show that projection of EEG dipole data onto MRI and PET may play a key role in the indication of surgery for the treatment of refractory epileptic patients, provided it is simple and easy to perform.

ACKNOWLEDGEMENTS

This work was supported in part by projects TIC99-1085-C002, CM 8.5/23/99, CM 08.1/049/98, CM III PRICYT and FIS-00/0036.

REFERENCES

1. B. J. Roth, M. Balish, A. Gorbach, and S. Sato, "How well does a three-sphere model predict positions of dipoles in a realistically shaped head?," *Electroencephalogr Clin Neurophysiol*, vol. 87, pp. 175-84, 1993.
2. B. N. Cuffin, D. L. Schomer, J. R. Ives, and H. Blume, "Experimental tests of EEG source localization accuracy in spherical head models," *Clin Neurophysiol*, vol. 112, pp. 46-51, 2001.
3. M. Scherg and T. W. Picton, "Separation and identification of event-related potential components by brain electric source analysis," *Electroencephalogr Clin Neurophysiol Suppl*, pp. 24.37, 1991.
4. E. Rodin, M. Rodin, R. Boyer, and J. Thompson, "Displaying electroencephalographic dipole sources on magnetic resonance images," *J Neuroimaging*, vol. 7, pp. 106-10, 1997.
5. B. Wang, C. Toro, T. A. Zeffiro, and M. Hallett, "Head surface digitization and registration: a method for mapping positions on the head onto magnetic resonance images," *Brain Topogr*, vol. 6, pp. 185-92, 1994.
6. S. S. Yoo, C. R. Guttmann, J. R. Ives, L. P. Panych, R. Kikinis, D. L. Schomer, and F. A. Jolesz, "3D localization of surface 10-20 EEG electrodes on high resolution anatomical MR images," *Electroencephalogr Clin Neurophysiol*, vol. 102, pp. 335-9, 1997.
7. B. H. Brinkmann, T. J. O'Brien, M. A. Dresner, T. D. Lagerlund, F. W. Sharbrough, and R. A. Robb, "Scalp-recorded EEG localization in MRI volume data," *Brain Topogr*, vol. 10, pp. 245-53, 1998.
8. I. Merlet, L. Garcia-Larrea, J. C. Froment, and F. Mauguiere, "Simplified projection of EEG dipole sources onto human brain anatomy," *Neurophysiol Clin*, vol. 29, pp. 39-52, 1999.
9. J. Sijbers, B. Vanrumste, G. Van Hoey, P. Boon, M. Verhoye, A. Van der Linden, and D. Van Dyck, "Automatic localization of EEG electrode markers within 3D MR data," *Magn Reson Imaging*, vol. 18, pp. 485-8, 2000.
10. V. L. Towle, J. Bolanos, D. Suarez, K. Tan, R. Grzeszczuk, D. N. Levin, R. Cakmur, S. A. Frank, and J. P. Spire, "The spatial location of EEG electrodes: locating the best-fitting sphere relative to cortical anatomy," *Electroencephalogr Clin Neurophysiol*, vol. 86, pp. 1-6, 1993.
11. I. Merlet, L. Garcia Larrea, M. C. Grégoire, F. Lavenne, and F. Mauguière, "Source propagation of interictal spikes in temporal lobe epilepsy. Correlations between spike dipole modelling and [18F]fluorodeoxyglucose PET data," *Brain*, vol. 119, pp. 377-92, 1996.
12. V. Diekmann, W. Becker, R. Jürgens, B. Grözinger, B. Kleiser, H. P. Richter, and K. H. Wollinsky, "Localisation of epileptic foci with electric, magnetic and combined electromagnetic models," *Electroencephalogr Clin Neurophysiol*, vol. 106, pp. 297-313, 1998.

13. T. D. Lagerlund, F. W. Sharbrough, C. R. Jack, Jr., B. J. Erickson, D. C. Strelow, K. M. Cicora, and N. E. Busacker, "Determination of 10-20 system electrode locations using magnetic resonance image scanning with markers," *Electroencephalogr Clin Neurophysiol*, vol. 86, pp. 7-14, 1993.
14. F. Maes, A. Collignon, D. Vandermeulen, G. Marchal, and P. Suetens, "Multimodality image registration by maximization of mutual information," *IEEE Trans Med Imaging*, vol. 16, pp. 187-98, 1997.
15. W. M. Wells, P. Viola, H. Atsumi, S. Nakajima, and S. Kikinis, "*Multi-modal volume registration by maximization of mutual information*," *Medical Image Analysis*, vol. 1, pp. 35-51, 1996/97.
16. M. Scherg, "Functional imaging and localization of electromagnetic brain activity," *Brain Topogr*, vol. 5, pp. 103-11, 1992.
17. W. H. Press, S. A. Teukolsky, W. T. Vetterling, and B. P. Flannery, *Numerical Recipes in C*, Second ed: Cambridge University Press, 1992.
18. F. Maes, D. Vandermeulen, and P. Suetens, "Comparative evaluation of multiresolution optimization strategies for multimodality image registration by maximization of mutual information," *Med Image Anal*, vol. 3, pp. 373-86, 1999.
19. T. Krings, K. H. Chiappa, B. N. Cuffin, J. I. Cochius, S. Connolly, and G. R. Cosgrove, "Accuracy of EEG dipole source localization using implanted sources in the human brain," *Clin Neurophysiol*, vol. 110, pp. 106-14, 1999.
20. N. S. Labs., "Curry. Multimodal Neuroimaging," : http://www.neuro.com/neuroscan/curry4.htm, 2000.